ELECTROCHEMICAL PERFORMANCE OF DOPED MnO$_2$ / GRAPHENE COMPOSITES

L. M. DONG[a, b*], K. X. SHI[a], L. G. JIN, Z. D. HAN[a,b], X. Y. ZHANG
[a]*College of Materials Science and Engineering, Harbin University of Science and Technology, Harbin 150080, China*
[b]*Key Laboratory of Graduate school of Engineering Dielectrics and Its Application, Ministry of Education, Harbin University of Science and Technology, Harbin 150080, China*

MnO$_2$ materials are prepared through a hydrothermal process. Sn-doping and composite graphene are both achieved simultaneously during the hydrothermal reaction then obtain the electrode materials of supercapacitors. Morphology, structure and electrochemical properties of the samples are evaluated by X-ray diffraction(XRD), scanning electron microscopy (SEM), and electrochemical work station. The results show that, the specific capacitance of 49 F·g^{-1}, 283 F·g^{-1} and 312 F·g^{-1} are exhibited for the pure MnO$_2$, Sn-MnO$_2$ and Sn-MnO$_2$ / graphene composite, respectively, indicating that stannum and graphene greatly enhances the electrochemical performance of MnO$_2$.

1. Introduction

With the rapid development of the global economy, the depletion of fossil fuels, and increasing environmental pollution, there is an urgent need for efficient, clean, and sustainable sources of energy, as well as new technologies associated with energy conversion and storage [1].Currently the most widely used for energy storage device are fuel cells, lithium ion battery, Dye-sensitized solar cells (DSSCs)[2]and supercapacitors. Supercapacitors, which are also called ultra capacitors or electrochemical double layer capacitors, are a kind of promising energy saving devices [3]. They have some advantages over batteries and fuel cells, including a short charge time, a wide operating temperature, long cycle life and high power density [4].Supercapacitors usually defined into electrochemical double layer capacitors (EDLCs) and pseudo-capacitors based on their different energy storage mechanisms [5].In recent years, transition metal oxides have received much attention for pseudo-capacitors since they could provide higher capacitance than carbon materials and longer cycle life than conductive polymers[6-16].

Among transition metal oxides, MnO$_2$ is one of the most promising electrode material for supercapacitors thanks to its high theoretical capacity, environmental compatibility, safety, abundant resources and cost effectiveness[17-18]. However, the poor electronic conductivity hindered its application [5]. Thus it is importance to employ effectively strategies to enhance the electronic conductivity of MnO$_2$. The common approach is doped other metal atoms into transition metal oxides. Since being K.S. Novoselov and A.K. Geim confirmed the presence of graphene[19], Owing to its large specific surface area, small resistivity, high electron mobility, and excellent

*Corresponding author: donglimin@hrbust.edu.cn

electrochemical stability, graphene has received much attention as a broad range of application in supercapacitors. In this study, MnO_2, $Sn-MnO_2$, and $Sn-MnO_2$ / graphene have been successfully synthesized by hydrothermal method. The performance of $Sn-MnO_2$ / graphene electrodes is compared with pure MnO_2 and $Sn-MnO_2$, and shows attractive high capacitive performance, implying the great potential of this material for high performance energy storage devices.

2.Experiment

2.1 Synthesis

MnO_2 is prepared by hydrothermal, the raw material: $KMnO_4$ (AR), $MnCl_2 \cdot 4H_2O$(AR),$n(KMnO_4)$: $n(MnCl_2)$ 2: 3 dissolved in deionized water, the molar ratio of $SnCl_4$ added were 1%, 2%, 5%, 10%, composite graphene, and was followed by the slow addition of $NH_3 \cdot H_2O$(AR), until pH = 7. After the hydrothermal reactor (Hydrothermal time 12h, Hydrothermal temperature 140℃),washed with deionized water and absolute alcohol for several times, and dried at 80 ℃ for 12 h in a vacuum oven, and then cooled to room temperature, grinded the sample, to obtain the desired active material. The electrode active material, acetylene black and polytetrafluoroethylene to 8: 1: 1 mixing ratio, transferred into a paste-like, coating on the surface of 2cm × 1cm nickel foam, and drying in a vacuum oven, until the quality of the electrode sheet became unchanged, to obtain the desired active electrodes.

2.2 Characterization

We use XRD determine the crystal structure of the sample, acquisition conditions: Cu target, the scanning speed of 10 / min, scanning range of 10 ° -80 °, use Sirion-200 model SEM , to determine the crystal surface morphology, then use RST5000 model Electrochemical Workstation determine the electrochemical performance of active electrode.

3. Results and Discusssion

3.1Morphology analysis

Fig. 1shows the surface morphology of the preparedMnO_2, $Sn-MnO_2$ and $Sn-MnO_2$ / graphene. Fig. 1 confirms that the three kinds of samples are the mixture of rod-like and granular. It can be clearly observed in Fig. b) and c) that the particle size become smaller, the reason may be that either adding stannum or composite graphene to form lattice distortion. The distortion degree of a axis direction and c axis direction are different, grain length to diameter ratio decreases, and the size of spherical particle is become smaller too. Therefore, the specific surface area of the electrode increases. Doping stannum and composite graphene as electrode material may offer significant synergistic effects arising from the larger surface area and high electrical conductivity of graphene.
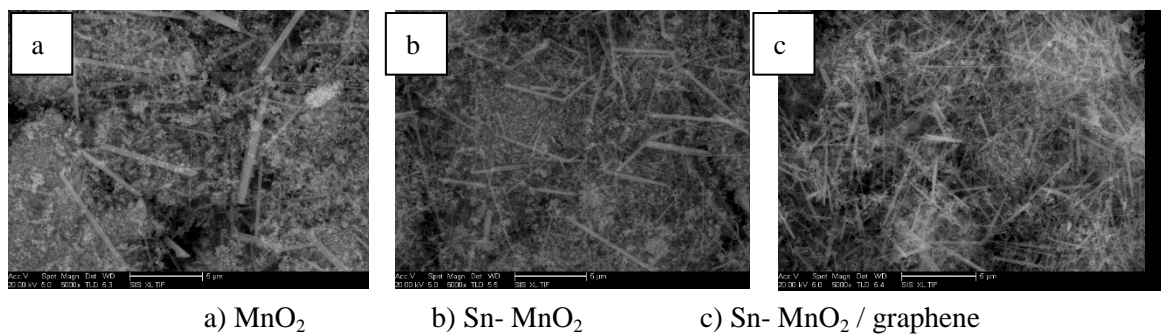
a) MnO$_2$ b) Sn- MnO$_2$ c) Sn- MnO$_2$ / graphene

Fig. 1 SEM images of MnO$_2$, Sn- MnO$_2$, Sn- MnO$_2$ / graphene

3.2 X-ray diffraction (XRD) analysis

Fig. 2 are X-ray diffraction patterns of MnO$_2$, Sn-MnO$_2$ and Sn-MnO$_2$ / graphene, the scan range of X-ray diffraction patterns is 10 ° ~ 80 °. XRD analysis of the as-synthesized samples showed the diffraction peaks at 28 °, 37 °, 41 °, 43 °, 57 °, 59 °, 65 °, 68 °and 72 °which were coincides with the standard PDF card 81-2261. As can be seen from Fig. 2, the XRD peak positions of Sn-MnO$_2$ and Sn-MnO$_2$ / graphene are similar with those of MnO$_2$, no obvious diffraction peaks of stannum or graphene were observed, indicating that adding stannum or composite graphene did not formed new phases, but formed a kind of solid solution, and therefore could not be detected the characteristic peaks of stannum or graphene in the XRD patterns. Furthermore, the XRD patterns of Sn-MnO$_2$ and Sn-MnO$_2$ / graphene show the weaker diffraction peaks. Due to lattice defects and distortion caused by adding stannum and composite graphene, he crystallinity of materials decreased, hence, the full width half maximum (FWHM) become wider, The average particle size of nanoparticles is estimated based on the Scherer Equation. Particle diameter (d) decreases with increase of FWHM, that consistent with the results of scanning electron microscopy.
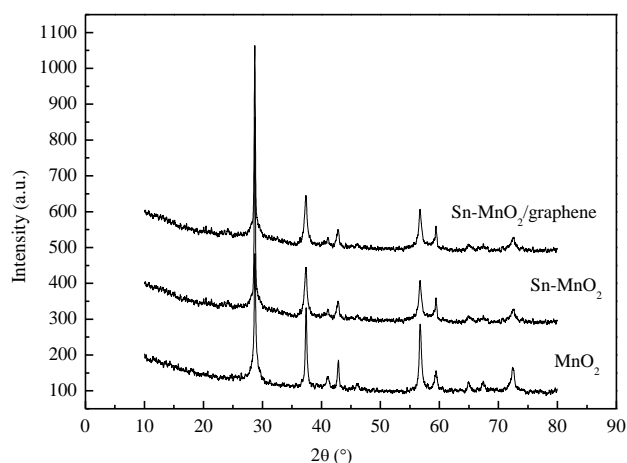

Fig. 2 XRD patterns of MnO$_2$, Sn-MnO$_2$, Sn-MnO$_2$ / graphene

3.3 Electrochemical properties of Sn-doped MnO$_2$

Fig.3 shows the cyclic voltammetry (CV) curves of Sn-doped MnO$_2$ between -0.1-0.9 V, under the scan rate of10 mV·s^{-1} in 0.5 M Na$_2$SO$_4$ electrolyte. Adding stannum amount of sample (a)–(e) are 0 mol%,1 mol%, 2 mol%, 5 mol%, 10 mol%, respectively. As can be seen from Fig.3, sample (c) electrodes yielded the largest current and resulted in much higher capacitance. Specific capacitance of electrodes(a), (b), (c), (d), (e) can be calculated by equation (1).

$$C_m = \frac{\int IdV}{s \times u \times m} \tag{1}$$

Where: C is the specific capacitance (F·g^{-1}), IdV is the integrated area of cyclic voltammetry, s is the scan speed (v·s^{-1}), $u$is the difference between the highest and lowest potential (V), and m is the mass of the active material in the electrodes (g). Results show that the specific capacitance of (a) is 49F·g^{-1}, (b) is 63 F·g^{-1}, (c) is 283 F·g^{-1}, (d) is 137 F·g^{-1}, and (e) is 113 F·g^{-1}. This results demonstrate that, Sn-MnO$_2$exhibits a much higher capacitive response than pure MnO$_2$,indicating that stannum doping enhances the electrochemical activity of MnO$_2$.With increasing the amount of stannum, the specific capacitance of electrodes showing a decreasing trend after increases. Due to the point defects in the crystal caused by the introduction of stannum, resulting in lattice distortion, so that migration of ions becomes easier, but MnO$_2$ itself has a large internal resistance, when the concentration of stannum is too large, it will cause lattice obstruction, hindering the ion transport, and the specific capacitance of electrode material decrease. Therefore, when adding stannum amount of 2 mol%, the specific capacitance of the electrode reaches the maximum, compare with pure MnO$_2$ increased by 478%.
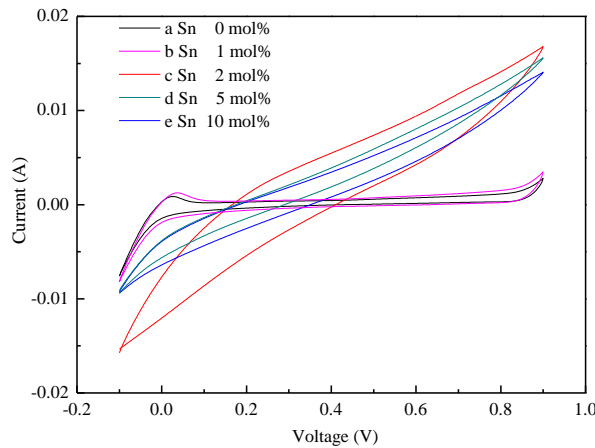

Fig. 3 Cyclic voltammetry of MnO$_2$ with different Sn content

Fig.4 shows the cyclic voltammetry curves over a voltage ranging from -0.1 to 0.9 V for Sn-MnO$_2$ with the amount of stannum is 2mol%, at different scan rates(10 mV·s^{-1},20 mV·s^{-1},50 mV·s^{-1}, and 100 mV·s^{-1}).It can be seen from Fig.4thatthe scan rate from 10 mV·s^{-1} to 20 mV·s^{-1} response current is proportional to the increase, indicating that the ion transport of electrode material can quickly performed, and the scan speed can maintain higher capacitance characteristics. However, when the scanning speed is increased from 20 mV·s^{-1} to 100 mV·s^{-1}, the response current is not greatly increased, due to the ion diffusion. From Fig. 4 it can also be seen from that, when the scan

rate increases, area of cyclic voltammetry curves gradually decreases, indicating that the electrode material is not suitable for use in high current. Meanwhile, the curve is gradually distorted from rectangular shape as the scan rate increases, demonstrating that the material does not have good reversibility, and the loss of capacitance is very big.
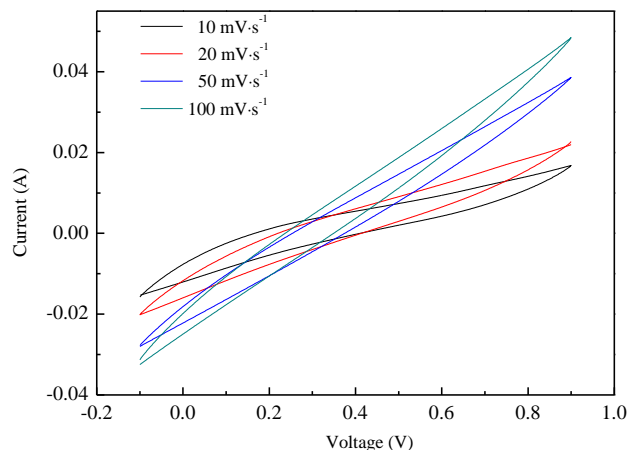

Fig. 4 Cyclic voltammetry of MnO_2 which have 2mol% Sn at different scanning speed

Fig.5 shows the AC impedance spectra of MnO_2 with different stannum content (0 mol%,1 mol%, 2 mol%, 5 mol%, 10 mol%).Frequency response characteristics and equivalent series resistance for assessing capacitance of supercapacitors are very important, because the impedance of the capacitor will reduce the charge storage potential range, weakening its charge storage capacity.Fig.5 shows that when the amount of stannum is less, the electrode series resistance (Rs)is decreases, improve the conductivity of the electrodes, which corresponds to the results of the cyclic voltammetry. However, when the amount of stannum excessive, can cause blockage of manganese dioxide, thereby hindering transfer of ions, and therefore Rs increases. In addition, in the low-frequency region both five kinds of samples plots present an oblique line, suggesting that the electrode process is under diffusion control. And the slope of the plot for MnO_2 with 2 mol% stannum is steeper than other, indicating that the material has excellent capacitance characteristics.
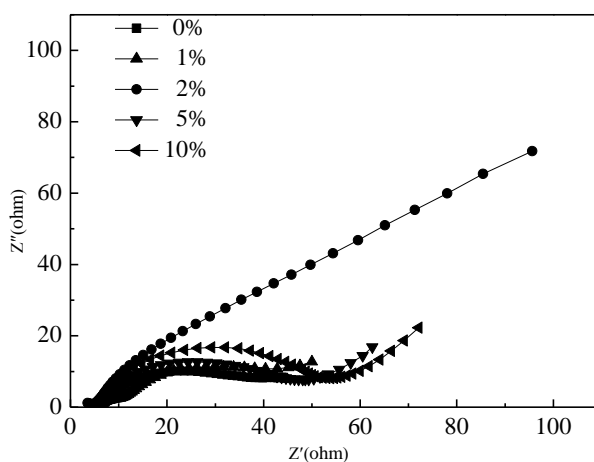

Fig. 5 AC impedance spectra of MnO_2 with different Sn content

3.4 Electrochemical properties of Sn-MnO2 / graphene composites

Fig. 6 shows the cyclic voltammetry (CV) curves of 2 mol% Sn-doped MnO2 between -0.1-0.9 V, under the scan rate of 10 mV•s-1 in 0.5 M Na2SO4 electrolyte. Compositing graphene amount of sample (a)–(e) are 0 mol%,1 mol%, 2 mol%, 5 mol%, 10 mol%, respectively. Specific capacitance of electrodes (a), (b), (c), (d), (e) can be calculated by equation (1).Calculation shows that when the amount of graphene for 5 wt.%, the specific capacitance of the composite material exhibits a higher capacitive behavior, up to 312 F•g-1, the specific capacitance compared with Sn-doped MnO2 increased by 10%, and compared with pure MnO2increased by 538 %,indicating that graphene can improve the electrochemical properties of the electrode material, owing to their unique two-dimensional structure, high surface area, remarkable chemical stability, and electrical conductivity.
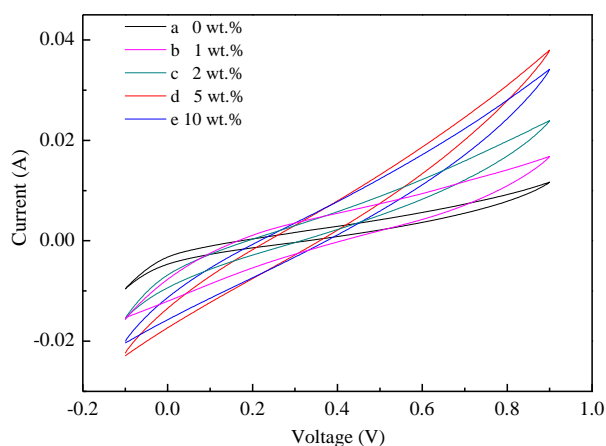

Fig. 6 Cyclic voltammetry of Sn-MnO$_2$/ graphene composites with different graphene content

Fig. 7 presents the cyclic voltammetry curves over a voltage ranging from -0.1 to 0.9 V for Sn -MnO$_2$ / graphene with the amount of stannum is 2 mol% and graphene is 5 wt.%, at different scan rates (10 mV·s^{-1}, 20 mV·s^{-1}, 50 mV·s^{-1}, and 100 mV·s^{-1}).It can be observed from Fig. 7 that the integrated area of the cyclic voltammetry curves no increased with increasing the scan rate, but decreased. As the scan rate increases, loss of energy increases and the stored charge on the electrode surface decreases causing the capacitance to decrease, indicating that the material is not suitable for working in high current. In addition, the shape of the cyclic voltammetry curves could not maintain the original shape but close to elliptical, demonstrating that the material have poor reversibility.
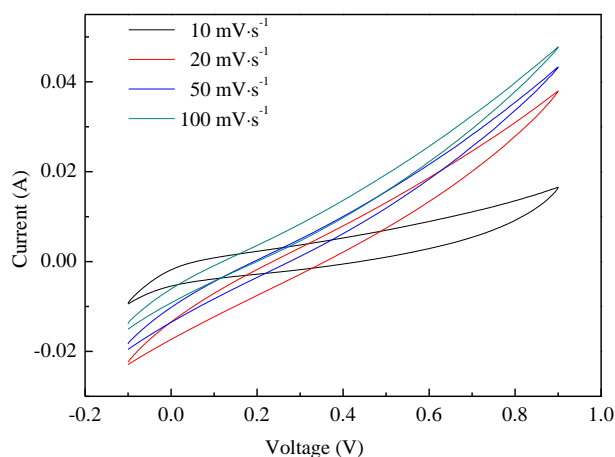
Fig. 7 Cyclic voltammetry of Sn-MnO$_2$ / graphene composites which have 5 wt.% graphene at different scanning speed

The electrochemical impedance spectroscopy analysis is an important technique for examining the fundamental behavior of electrode materials for supercapacitors. The AC impedance plots for Sn-MnO$_2$ / graphene composite electrodes with different graphene content (0 wt.%,1 wt.%,2 wt.%,5 wt.%,10 wt.%) are shown in Fig.8. As can be seen fromFig.8, at high-frequency, the intercept of the real part (Z$'$) for pure Sn-doped MnO$_2$is larger than others. The plots are composed of a line in the low-frequency region. It should be noted that the amount of graphene is 2 wt.% or 5 wt.%, the slope of electrode material is bigger, indicating a better capacitive behavior. This result may be due to the addition of the high surface area of the graphene, which enhances the conductivity of the composites. However, it should also be noted that the electrode materials may tend to form irreversible agglomerates or graphene sheets overlap each other, hindering transfer of ions due to the excessive adding of graphene.
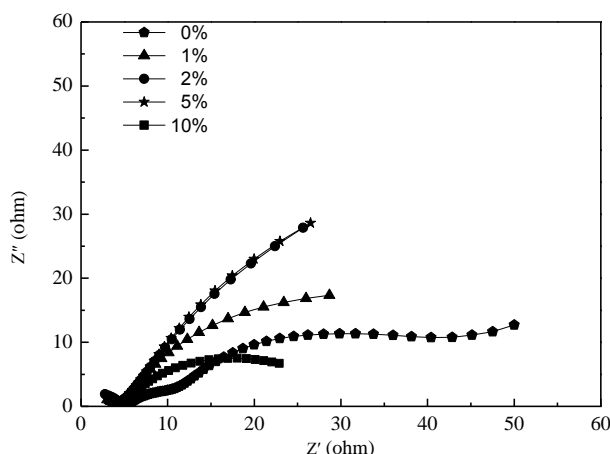

Fig. 8 AC impedance spectra of Sn-MnO$_2$ / graphene composites with different graphene content

4. Conclusions

In this study, MnO$_2$, Sn-MnO$_2$, andSn-MnO$_2$ / graphene composites were successfully fabricated using hydrothermal method. The specific capacitance of 49 F·g^{-1}, 283 F·g^{-1} and 312 F·g^{-1} are displayed for the pure MnO$_2$, Sn- MnO$_2$ and Sn-MnO$_2$ / graphene composite, respectively. In

comparison, the Sn-MnO$_2$ / graphene composites exhibited much better electrochemical performance in terms of capacitance than pure MnO$_2$ and Sn-MnO$_2$.We found that the electrode materials using 5 wt.% graphene composited and 2 mol% Sn-doped provide the highest specific capacitance of 312 F·g^{-1} is due to the high conductive of graphene, large surface of Sn-doped and graphene which makes the Sn-MnO$_2$ / graphene composites possible to use in the supercapacitors. We also found that the right amount of stannum and graphene is necessary, excess or insufficient will reduce the electrical properties of the electrode material.

Acknowledgements

References

[1] G. P. Wang, L. Zhang, J. J. Zhang, Chemical Society Reviews,**41**(2),797(2012).

[2] L. G.Jin, Z. Wu, T. X. Wei, J.Zhai, X. Y. Zhang, ChemCommun, **47**, 997(2011).

[3] Q. Cheng, J. Tang, J. Ma, H. Zhang,N. Shinya, L. C. Qin, Carbon,**49**, 2917(2011).

[4] H. W. Yu, J. J. He, L. Sun, S. Tanaka, B. Fugetsu, Carbon, **51**, 94(2013).

[5] Y. Z. Wu, S. Q. Liu, H. Y. Wang, X. Y. Wang, X. Zhang, G. H. Jin, Electrochimica Acta,**90**, 210(2013).

[6] V. D. Patake, C. D. Lokhande, O.S.Joo, Applied Surface Science,**255**(7), 4192(2009).

[7] K. C. Liu, M. A. Anderson, Electrochemical Society,**143**(1), 124(1996).

[8] K.W.Nam, K. B.Kim, Electrochemical Society, **149**(3),346(2002).

[9] M. Q. Wu, J. H. Gao, S. R. Zhang, Journal of Porous Materials,**13**(3),7(2006).

[10] Y. G. Zheng, M. L. Zhang. Materials Letters, **61**(18), 967(2007).

[11] J. Lee, G. Kim, K.Kim, Journal of Nanoscience and Nanotechnology, **10**(5),676(2010).

[12] S. L. Xiong, C.Z. Yuan, X. G. Zhang, B. J. Xi, Y. T. Qian, Chemistry-a European Journal, **15**(21),320(2009).

[13] J. Xu, L. Gao, J. Y. Cao, W. C. Wang, Z. D.Chen, ElectrochimicaActa,**56**(2),32(2010).

[14] C. C. Hu, C. M. Huang, K. H. Chang, Journal of Power Sources,**185**(2), 1594(2008).

[15] Z. Chen, V. Augustyn, J. Wen, Y. W. Zhang, M. Q. Shen, B. Dunn, Y. F. Lu, Advanced Materials, **23**(6), 791(2011).

[16] X. P. Zhou, H. Y. Chen, D. Shu, C. He, J. M. Nan, Physics and Chemistry of Solids, **70**(2), 495(2009).

[17] Q. Li, Z. L. Wang, G. R. Li, R. Guo, L. X. Ding, Y. X. Tong, Nano letters, **12**(7), 3803(2012).

[18] K. Dai, L. H. Lu, C. H. Liang, J. M. Dai, Q. Z. Liu, Y. X. Zhang, G. P. Zhu, Z. L. Liu, Electrochimica Acta, **116**, 111(2014).

[19] K. S. Novoselov, A. K. Geim, S. V. Morozov, D. Jiang, Y. Zhang, S. V. Dubonos, I. V. Grigorieva, A. A.Firsov,Science,**306**, 666(2004).